Journal of Materials Chemistry B

Materials for biology and medicine

www.rsc.org/MaterialsB

Volume 1 | Number 38 | 14 October 2013 | Pages 4867–5164

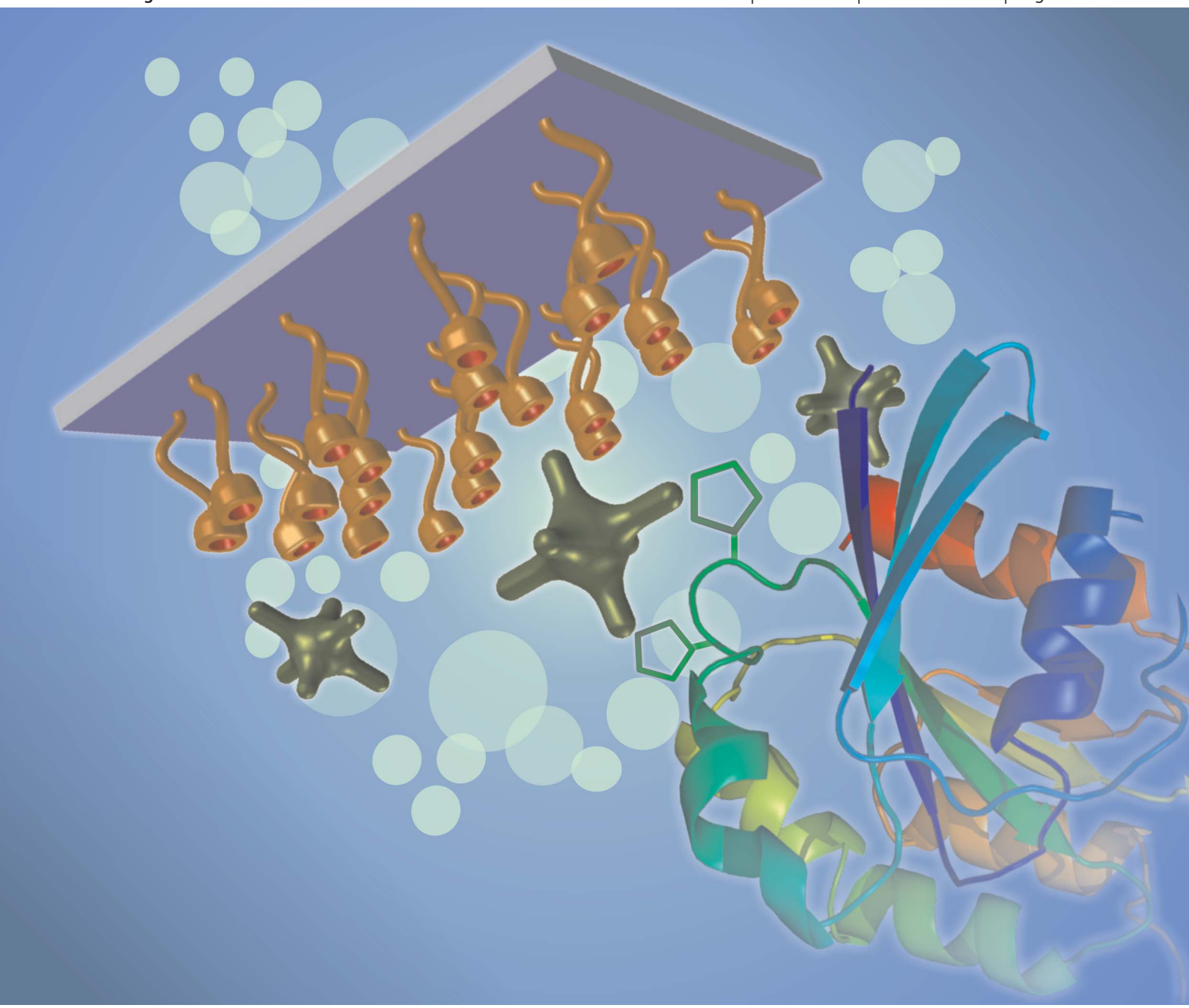

ISSN 2050-750X

RSC Publishing

PAPER

Carla E. Giacomelli *et al.*

Ni(II)-modified solid substrates as a platform to adsorb His-tag proteins

2050-750X(2013)1:38;1-O

Journal of Materials Chemistry B

RSC Publishing

PAPER

Ni(II)-modified solid substrates as a platform to adsorb His-tag proteins†

Cite this: *J. Mater. Chem. B*, 2013, **1**, 4921

Laura E. Valenti,‡[a] Vitor L. Martins,‡[b] Elisa Herrera,[a] Roberto M. Torresi[b] and Carla E. Giacomelli*[a]

Received 31st May 2013
Accepted 19th July 2013

DOI: 10.1039/c3tb20769b

www.rsc.org/MaterialsB

This work investigated a simple and versatile modification to a solid substrate to develop electrochemical bio-recognition platforms based on bio-affinity interactions between histidine (His)-tagged proteins and Ni(II) surface sites. Carboxylate (COO)-functionalized substrates were prepared in multiple steps, initiated with an amino-terminated self-assembled monolayer (SAM) on polycrystalline gold. Surface enhanced Raman spectroscopy (SERS), quartz crystal microbalance with dissipation monitoring (QCM-D) and contact angle measurements were used to follow the modification process. Upon completion of the modification process, the surface COO–Ni(II) chelate complex and the coordination mode used to bind the His-tag proteins were characterized by X-ray absorption near-edge spectroscopy (XANES). Finally, the electrochemical stability and response of the modified substrates were evaluated. The versatility of the modification process was verified using silica as the substrate. QCM-D and SERS results indicated that two types of films were formed: a COO-terminated SAM, which resulted from the reduction of previously incorporated surface aldehyde groups, and a physically adsorbed polymeric glutaraldehyde film, which was produced in the alkaline medium. XANES spectral features indicated that COO–Ni(II) formed a non-distorted octahedral complex on the substrate. The electrochemical stability and response towards a redox mediator of the COO–Ni(II)-terminated SAM indicated that this platform could be easily coupled to an electrochemical method to detect bio-recognition events.

Introduction

Solid substrates (*e.g.*, electrodes, chips and (nano)particles) modified with metal cations (*e.g.*, Ni(II), Cu(II), Co(II) or Zn(II)) have been used for a wide variety of applications including protein purification,[1] bio-functional surfaces,[2–4] cell recognition behavior,[5] controlled drug release[6] and electron transfer reactions in enzymes.[7] The metal cations are usually incorporated by grafting a chelating agent on the sorbent surface, such as nitrilotriacetic acid (NTA), iminodiacetic acid (IDA) and EDTA, that partially coordinates the cations. Due to the high affinity of this surface chelate complex for the polyhistidine (usually hexahistidine, His_6)-tagged protein,[8] this substrate modification is intended to preferentially adsorb site-oriented His-tag proteins.[9] One of the major advantages of this strategy is that it enables the tag to be genetically introduced into recombinant proteins without disrupting the native and biologically active structure. Hence, the preferred orientation is induced by incorporating the tag at one of the termini (N or C) or in an exposed loop of the protein. Many commercially available protein expression plasmid vectors incorporate the His-tag in the primary sequence for recombinant protein purification facilitating the use of His-tag proteins with diverse applications. The bio-affinity of the reaction between metal cations and His residues provides a gentle site-oriented adsorption procedure that has several important advantages over other strategies: (a) the attachment is site-specific relative to the location on the protein sequence where the bond with the sorbent substrate forms; (b) the adsorption conditions are mild, which result in a reduced risk of protein denaturation; (c) the protein molecules have one orientation and the adsorbed layer is homogeneous; and (d) the sorbent substrate is reusable.

The chelating agent may be covalently attached on functionalized substrates or included as a reactive terminal group of the molecular units composing self-assembled monolayers (SAMs) (*e.g.*, thiols on gold or organosilanes on silica).[10] SAMs

[a]*Instituto de Investigaciones en Físico Química de Córdoba (INFIQC) CONICET-UNC, Departamento de Fisicoquímica, Facultad de Ciencias Químicas, Universidad Nacional de Córdoba, Ciudad Universitaria, X5000HUA Córdoba, Argentina. E-mail: giacomel@fcq.unc.edu.ar*

[b]*Instituto de Química – Universidade de São Paulo, Av. Prof. Lineu Prestes 748, 05508-000 São Paulo, SP, Brazil*

† Electronic supplementary information (ESI) available: The figures of the QCM-D *in situ* response for the five steps involved in the modification of gold in the presence of cysteamine up to KNO_3 rinsing (Fig. S1) and in the absence of cysteamine up to either histidine or KNO_3 rinsing (Fig. S2), the addition of Ac_2O to Au/Cyst and gold substrates (Fig. S3), voltammograms of the Au/Cyst electrode for different potential cycles (Fig. S4) and XANES spectra of the Ni(II) surface complexes on a gold substrate at different applied potentials (Fig. S5) are shown. See DOI: 10.1039/c3tb20769b

‡ Both authors contributed equally to this manuscript.

on gold substrates are often used because the distance between the protein and the substrate can be tuned by changing the length of the thiol, and the use of thiols with different terminal groups can change the density of the protein layer. Moreover, gold substrates are widely used in different techniques such as quartz crystal microbalance (QCM),[5,11] surface plasmon resonance (SPR),[6] and electrochemical methods,[7] which are used to study proteins at interfaces, detect bio-recognition events or evaluate enzymatic electron transfer reactions. Two methods are currently used to generate chelating layers on SAM-modified gold substrates: (1) a single-step method based on the assembly of designed and synthesized chelate-terminated thiols[2–7,12] and (2) a multi-step method based on grafting the chelating moiety onto a pre-assembled SAM with exposed reactive groups.[11,13] Although both methods have advantages and disadvantages, multi-step modification does not require tedious purification of the synthesized molecules, is easily applied to micro- and nano-arrays, can be extended to other substrates by changing the first reactive layer that is assembled, and is easily complemented with other moieties (*e.g.*, oligoethylene glycol) by adding an additional step during the modification process.

Several publications have reported the preparation, characterization and binding properties of solid substrates modified with chelating moieties. These proposed surface complexes with metal cations comprise the carboxylate and amino groups of polydentate ligands. As an example, it has been suggested that a Ni(II) ion is coordinated to one NTA molecule (3O, 1N) and two water molecules that are replaced by the histidine residues of the His-tag proteins.[1,13] Based on this coordination mode, carboxylate (COO)-functionalized substrates may act as cation chelating substrates as well. Herein, COO-functionalized substrates are proposed to be used as an alternative method to develop bio-functional surfaces based on the bio-affinity interaction between His-tag proteins and Ni(II) modified solid substrates. In the first place, COO-functionalized polycrystalline gold was prepared in multiple steps, initiated with an amino-terminated (*e.g.*, cysteamine) SAM, to be used as surface electrochemical bio-recognition platforms. The versatility of the modification process was demonstrated by substituting gold for silica as the substrate and cysteamine for 3-aminopropyltrimethoxysilane in the first step of the substrate modification process. The electrochemical platforms were prepared on polycrystalline gold that represents the most used substrate to prepare bio-functional surfaces. Further, their characterization and performance was followed in aqueous solution, compatible with real biological environments. To this end, this work studied the following: (a) each step of the substrate modification process using surface enhanced Raman spectroscopy (SERS), quartz crystal microbalance with dissipation monitoring (QCM-D) and contact angle measurements, (b) the coordination mode of the Ni(II)–surface chelate complex upon addition of the His-tag by X-ray absorption near-edge spectroscopy (XANES) at the Ni–K edge in aqueous solution, and (c) the electrochemical stability and response of the modified substrate by cyclic voltammetry (CV). To the best of our knowledge, this work represents the first report regarding Ni(II)-modified substrates studied using XANES in an aqueous solution focused on the metal cation. Most studies that used XANES to investigate SAM-modified gold were performed under high vacuum conditions at the C or O edge.[3,14] However, several Ni(II) coordination compounds with different ligands were previously studied using XANES in aqueous solutions.[15–20]

Experimental

Reagents

3-Aminopropyltrimethoxysilane (APTMS) was supplied by Sigma; cysteamine (Cyst) and $NaBH_4$ from Fluka; absolute ethanol, acetic anhydride (Ac_2O), acetic acid, pyridine, $(NH)_4OH$, histidine (His), and imidazole (Imi) from Anhedra; glutaraldehyde (Glut), $Ni(NO_3)_2 \cdot 6H_2O$, $NaH_2PO_4 \cdot 7H_2O$ and NaCl from Baker; and hexahistidine (His_6, 98.4% purity) from New England Peptide, Inc. All reagents were of analytical grade and used without further purification. Aqueous solutions were prepared in deionized water (Milli Q System, Millipore). The pH measurements were performed with a glass electrode and a digital pH meter (Orion 420 A+, Thermo). All experiments were performed at room temperature (26 ± 2 °C).

Substrates

The polycrystalline gold substrates (99.99% purity) were 0.3 mm thick plates with dimensions of 0.5 × 1.5 cm, while 100 nm thick layers of silica were prepared by oxidizing 100 mm silicon wafers (Silicon Valley Microelectronics Inc., Santa Clara, CA, USA) at 1000 °C for 1 hour.[21] To have a clean surface before use, both substrates were immersed in a boiling piranha solution (H_2SO_4–H_2O_2 3 : 1) for 30 minutes, rinsed thoroughly with deionized water and dried under an N_2 flow. (**Caution!** Piranha solution is a powerful oxidizing agent that reacts violently with organic compounds; it should be handled with extreme care.) Silica substrates were further treated with air plasma (Harrick Plasma) for 20 minutes to increase the surface reactivity.[22] The substrates were used immediately after completion of the cleaning procedure.

Quartz crystals (AT-cut) with 100 nm gold layer sensors (QSX-301) were purchased from Q-Sense, with a fundamental resonance frequency of 4.95 MHz. For cleaning purposes, the sensors were immersed in a H_2O_2–NH_4OH–H_2O (1 : 1 : 5) solution at 70 °C for 5 minutes, rinsed with deionized water, sonicated in both deionized water and ethanol for 5 minutes each, dried under an N_2 stream and cleaned with UV/ozone (ProCleaner Bioforce Nanoscience) for 15 minutes. The sensors were used immediately after completion of the cleaning procedure.

Methods

Substrate modification. COO gold substrates were prepared in multiple steps, which began with the formation of an amino-terminated SAM as schematically depicted in Fig. 1. For this step, gold substrates were incubated in a 20 mmol L^{-1} cysteamine solution (absolute ethanol) overnight (Au/Cyst). In the second step, the amino-modified substrates were incubated in 5% w/v glutaraldehyde (10 mmol L^{-1} pyridine buffer at pH 9.0)

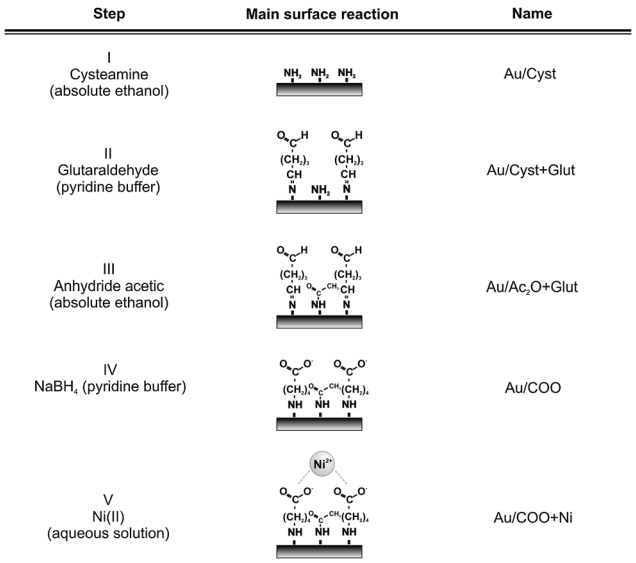

Fig. 1 Schematic representation of the main surface reactions involved in the five steps used to modify the gold substrates: (I) immersion of the substrate in a solution of 20 mmol L^{-1} cysteamine in absolute ethanol overnight; (II) immersion of the substrate in a solution of 5% w/v glutaraldehyde in 10 mmol L^{-1} pyridine buffer at pH 9.0 for 2 hours; (III) immersion of the substrate in a solution of 10% v/v Ac_2O in absolute ethanol for 30 minutes; (IV) immersion of the substrate in 0.02 mg mL^{-1} aqueous solution of $NaBH_4$ for 5 hours at 4 °C; and (V) immersion of the substrate in a 1.0 mol L^{-1} Ni(II) aqueous solution.

for 2 hours (Au/Cyst + Glut), which was followed by incubation of the Au/Cyst + Glut in a 10% v/v Ac_2O solution (absolute ethanol) for 30 minutes (Au/Glut + Ac_2O). After the SAM formation and Ac_2O reaction, the substrates were rinsed with absolute ethanol followed by the pyridine buffer. After the glutaraldehyde reaction, the rinsing steps were performed in the reverse order. In the fourth step, Au/Glut + Ac_2O was incubated in a fresh aqueous $NaBH_4$ solution (0.02 mg mL^{-1} final concentration) for 5 hours at 4 °C and rinsed with the pyridine buffer and deionized water (Au/COO). Finally, the substrates were stored in 1.0 mol L^{-1} $Ni(NO_3)_2$ until further use (Au/COO + Ni). The same procedure was used for the silica substrates (SiO_2/COO + Ni), except that the first step was performed in a 1% v/v APTMS solution (absolute ethanol) for 2 hours.

To induce the specific interaction between the surface COO–Ni(II) complex of the substrate and either His_6 (substrate/COO + Ni + His_6), His (substrate/COO + Ni + His) or Imi (substrate/COO + Ni + Imi), the substrates were incubated in a 1.2 mmol L^{-1} His_6, 0.2 mol L^{-1} His or 0.5 mol L^{-1} Imi solution (5 mmol L^{-1} phosphate buffer at pH 8.0) for 20 minutes, and then rinsed with the buffer solution prior to performing measurements.

Surface enhanced Raman spectroscopy. The SERS spectra were obtained with a Horiba – Jobin Yvon spectrometer (LABRAM-HR). A liquid-nitrogen-cooled charge coupled device (CCD) detector (Jobin Yvon, model CCD3000) was used in these measurements. A spectral resolution of 4 cm^{-1} was used. The 514 nm line of an Ar-ion laser and the 632 nm line of a He/Ne laser were used as the excitation sources in the 500–2000 cm^{-1} range. The laser power at the sample was set at 3.5 mW. Special care was taken to monitor whether the laser power damaged the sample or caused desorption from the Au substrate.

The SERS spectra of each modification step were collected twice with different Au substrates. The spectra were baseline and blank (bare gold spectrum) corrected. The original spectra were smoothed using the Savitsky–Golay 5 points smoothing procedure.

To improve the SERS signals, the bare gold substrates were electrochemically treated in H_2SO_4 to increase the surface roughness, as described elsewhere.[23,24]

Quartz crystal microbalance with dissipation and contact angle measurements

The QCM-D experiments were performed for each substrate modification step by Q-Sense E4 in a flow cell module. The changes in resonance frequency (Δf_n) and dissipation (ΔD_n), where n denotes the recorded overtones (5, 7, 9 and 11), were simultaneously monitored. All measurements were performed at 25 °C. Before and after each modification step, the solvent used during the reaction was allowed to flow through the cell until Δf_n and ΔD_n stabilized. All steps were performed at a flow rate of 200 μL min^{-1} except the overnight step that involved cysteamine, which was performed at a flow rate of 50 μL min^{-1}. Changes in the resonance frequency can be related to the changes in mass (Δm) using the Sauerbrey equation:[25]

$$\Delta f_n = -\left(\frac{2 f_n^2}{n^2\sqrt{\mu\rho}}\right)\frac{\Delta m}{A} = -\frac{\Delta m}{C \times A} \quad (1)$$

where Δf is the measured shift in frequency (Hz), A is the active area of the crystal corresponding to the exciting electrode exposed to the working environment, ρ is the quartz density (2.648 g cm^{-3}), μ is the shear modulus (2.947×10^{11} g cm^{-1} s^{-2}) and f_n is the crystal frequency for the n overtone (5 MHz for the fundamental tone). The theoretical mass sensitivity (C) was calculated by using the quartz crystal parameters and the value was 17.7 ng cm^{-2} Hz^{-1}. In order to confirm the mass sensitivity value, experiments of copper electrodeposition were performed in 0.1 mol L^{-1} of $CuSO_4$ in 0.5 mol L^{-1} H_2SO_4 aqueous solution at six different polarization currents. The C value obtained was 17.9 ± 0.5 ng cm^{-2} Hz^{-1} which is in agreement with the theoretical value. A decrease in the resonance frequency indicates that the mass is increased. Changes in ΔD_n are related to the viscoelastic properties of the film.

The quartz crystal was dried under an N_2 stream and the contact angle of a 5 μL deionized water droplet on the modified substrate was measured at various stages of the substrate modification using a GBX Instrumentation Scientifique coupled to a Nikon-PixeLINK camera. The software PixeLINK Capture OEM (v. 7.12) and Visiodrop GBX (v. 1.02.01.01) were used.

X-ray absorption near-edge spectroscopy

The X-ray absorption near-edge spectroscopy (XANES) data at the Ni–K edge of the surface complexes (either on gold or silica) in the 5 mmol L^{-1} phosphate buffer at pH 8.0 were collected in the fluorescence mode, while the spectra in aqueous solutions (references) were acquired in the transmittance mode.

Table 1 Reference complexes for XANES measurements. Charges and water molecules are omitted in the complexes

Ligand (experimental conditions)	Species studied by XANES (involved groups in coordination)	References
H_2O	$Ni(OH_2)_6$ ($6OH_2$)	
NH_3 (NH_4OH excess, pH > 11.0)	$Ni(NH_3)_6$ ($6NH_3$)	43
Imidazole (Imi) (M : L ratio 1 : 6, pH 8.0)	45% $Ni(Imi)_4$ (4 $-N_{(Imi)}$, $2OH_2$) 25% $Ni(Imi)_5$ (5 $-N_{(Imi)}$, $1OH_2$) 20% $Ni(Imi)_3$ (3 $-N_{(Imi)}$, $3OH_2$) 10% $Ni(OH_2)_6$	43
Histidine (His) (M : L ratio 1 : 2, pH 8.0)	$Ni(His)_2$ (2 –OOC–, 2 $-NH_2$, 2 $-N_{(Imi)}$)	44
Hexahistidine (His_6) (M : L ratio 1 : 1, pH 5.0)	$Ni(His_6)H$ (1 $-N_{(Imi)}$, 1 $-N_{(Amida)}$, $4OH_2$)	44
Acetate ion (AA) (acetic acid excess, pH > 5.0)	40% Ni(AA) (1 –OOC–, $5OH_2$) 40% $Ni(AA)_2$ (2 –OOC–, $4OH_2$) 20% $Ni(OH_2)$	52

Reference solutions were prepared with the metal-to-ligand ratios and pH values listed in Table 1, which also includes the species present in solution. Measurements were conducted at the XAS beam line of the National Synchrotron Light Source (LNLS), Brazil. The data acquisition system for XAS was comprised of four X-ray detectors (incident I_o, transmitted I_t, reference I_r, and fluorescence). The reference channel was employed primarily for internal calibration of the edge position using pure Ni foil. The low critical energy of the LNLS store ring (2.08 keV) led to the expectation that the third order harmonic contamination of the Si(111) monochromatic beam was negligible above 5 keV.[26]

The Athena package was used for the analysis of the X-ray absorption data. The XANES spectra were first corrected for background absorption by fitting the pre-edge data (*i.e.*, −60 to −20 eV below the edge) to a linear formula, followed by extrapolation and subtraction of the background from the data over the energy range of interest. Next, the spectra were calibrated for the edge position using the second derivative of the inflection point at the edge jump of the data from the reference channel. To determine the position of the absorption edge, the energy value corresponding to a normalized absorbance of 0.5 was used. The XANES reference spectra were treated similarly to the spectra obtained from the fluorescence mode. To evaluate the effects of the applied potential on the chemical modification, the system was connected to a potentiostat/galvanostat 173 EG&G PARC coupled to a signal generator 175 EG&G PARC, on which the modified gold substrate was used as the working electrode, $Ag/AgCl/KCl_{sat}$ was used as the reference electrode, and a Pt wire was used as the counter electrode.

Cyclic voltammetry

CV experiments were performed using a potentiostat/galvanostat Autolab PGSTAT 30 (Ecochemie). Either bare or modified (up to different stages) gold substrates were used as the working electrode, $Ag/AgCl/KCl_{sat}$ was used as the reference electrode and a Pt wire was used as the counter electrode, which were immersed in a 50 mmol L^{-1} phosphate buffer at pH 8.0. The electrochemical stability of the SAM was determined by applying potential cycles between −1.00 and 1.25 V at a scan rate of 100 mV s^{-1} in the positive and negative directions. To study the electrochemical stability of gold at different modification stages, various scans were performed between 0.00 and 0.70 V at 100 mV s^{-1}. To compare the electron transfer capabilities of bare and modified gold, CV experiments were performed in a 2.5 mmol L^{-1} (dimethylaminomethyl)ferrocene solution (50 mmol L^{-1} phosphate buffer at pH 8.0) between 0.00 and 0.50 V at 100 mV s^{-1}.

Results and discussion

Ni(II) layer assembly

Fig. 1 schematically illustrates the five steps used for the modification of the gold substrate; the functional groups added or removed during each one of these steps were evaluated by SERS as shown in Fig. 2. Fig. 2A displays the spectral range corresponding to the characteristic bands due to C–S stretching vibrations of adsorbed cysteamine on gold[27,28] for the first two modification steps. On the other hand, Fig. 2B shows a wider range where all the functional groups of the four modification steps before adding Ni(II) give the SERS signal (in both figures the spectra were shifted in the *y* axis for clarity providing the spectrum of the first step of the modification at the bottom and that of the last one on top of the figure). All the spectra showed

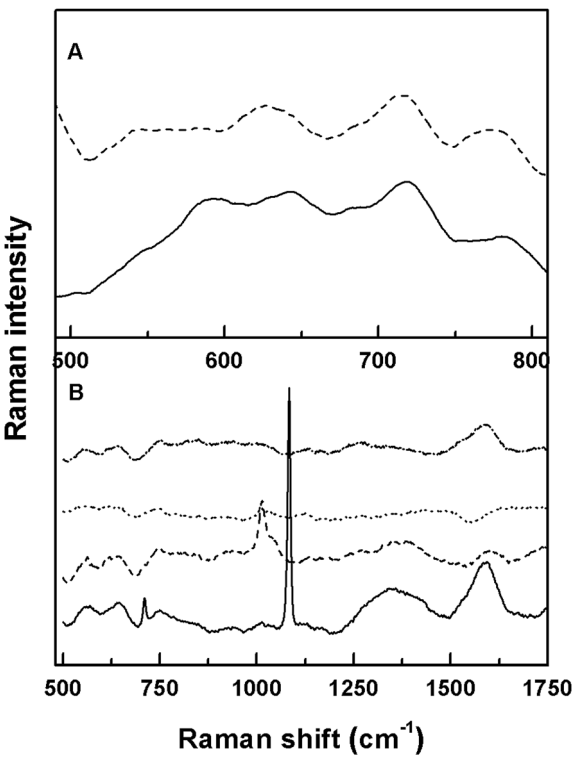

Fig. 2 SERS spectra for the different steps of the modification substrate. Step 1 (solid line), step 2 (dashed line), step 3 (dotted line) and step 4 (dashed–dotted line). (A) He–Ne 632 nm laser in the range of 500–800 cm^{-1}. (B) Ar ion 514 nm laser in the range of 500–1750 cm^{-1}.

broad bands typical of adsorbed molecules on polycrystalline substrates. Considering the strong dependence of SERS signals on the orientation of the adsorbed molecules, this spectral feature indicated that the adsorbed functionalities adopted slightly different orientation on the polycrystalline substrate. According to the allocation of SERS signals of cysteamine, amino acids and sulfur containing homodipeptides on gold substrates, these broad bands can be divided into four regions ranging between 500 and 1750 cm^{-1}:[27–30] (a) 500 cm^{-1} and 900 cm^{-1} assigned to the ν(S–C) (as indicated in Fig. 2A), (b) 1000 cm^{-1} and 1160 cm^{-1} due to the vibrations of the R–NH_2 group, (c) 1200 cm^{-1} and 1400 cm^{-1} assigned to the overlapping vibrations of different functionalities ($\varpi(CH_2)$, δ(C–C–H), ν(C–NH_2) and ν(COOH)) and (d) 1480 cm^{-1} and 1670 cm^{-1} assigned to the overlapping stretching vibrations of different bonds (C═O, C═N and C–N–C).

The observed signals of the adsorbed cysteamine on gold in the spectrum of the first modification step in Fig. 2A (bottom) were attributed to the *trans* and *gauche* conformations of the S–C–C chain.[27] The bands at lower frequencies (between 620 cm^{-1} and 650 cm^{-1}) correspond to the stretching vibration of the *gauche* conformer while the band at around 730 cm^{-1} indicates the presence of the *trans* conformer.[28] The *gauche* conformer has been usually observed on gold substrates due to its strong interaction with the nitrogen atom of the amine group. This conformation may hamper further surface reactions of this functional group. However, the ratio between the intensities of the *gauche*/*trans* bands decreases in the spectrum (top) of the second step of the modification suggesting that the glutaraldehyde addition induced a conformation change towards the *trans* conformer. Fig. 2B shows that the signals attributed to the C–S stretching vibrations are present in the spectra of the different modification steps demonstrating that the cysteamine SAM was strongly attached to the gold substrate. It is important to note that some publications have proposed the use of $NaBH_4$ to remove alkanethiols from gold.[31] However, the concentration of the $NaBH_4$ solution and the dipping time and temperature used during step IV did not affect the first modification layer.

In addition to ν(C–S), bands between 1000 cm^{-1} and 1160 cm^{-1} assigned to the amino group of cysteamine are present in the spectrum of the first modification step (bottom of Fig. 2B). In fact, the strongest signal at 1086 cm^{-1} corresponds to the ν(C–C–N) which is due to the interaction between the nitrogen atom and the gold substrate of the *gauche* conformer, as also observed with cysteine on gold.[30] This signal diminishes and shifts towards lower wavenumber (1013 cm^{-1}) in the spectrum of the second step of the modification, supporting the *gauche*/*trans* transition of the adsorbed cysteamine upon glutaraldehyde addition. Further, the presence of this band indicates that a fraction of the amino groups did not react during the second step of the modification. In fact, this SERS signal only disappeared in the spectrum of the third modification step which was intended to block the unreacted surface amino group with Ac_2O. Although the SERS signal of the imine bond[29] produced by the reaction between the amino and aldehyde groups is not resolved in the broad band between 1480 cm^{-1} and 1670 cm^{-1} in the spectrum of the second modification step, the splitting of the band at 1369 cm^{-1} in the spectrum of the first modification step band accounts for this reaction. This spectral change gives a weak band at around 1400 cm^{-1} assigned to the surface carboxylate groups ($\nu(COO^-)$),[32] which were produced by the partial oxidation of the aldehyde functionality, and another one at around 1300 cm^{-1} related to δ(C–C–H). The low intensities of these bands along the modification steps indicate that the COO^- groups were not in the proximity of the gold substrate. In short, the reaction between the surface amino groups and the glutaraldehyde in the second modification step produced a change in the orientation of the adsorbed cysteamine and a partial incorporation of the carboxylate functionality pointing towards the solution. Blocking the unreacted surface amino groups with Ac_2O in the third step of the modification resulted in neutral carboxyl methyl surface groups.[33] Finally, $NaBH_4$ was added to reduce the unstable imine bond to the more stable amine one. However, this reaction was not observable by SERS because the vibration of these bonds was overlapped with the broad band between 1480 and 1670 cm^{-1}.

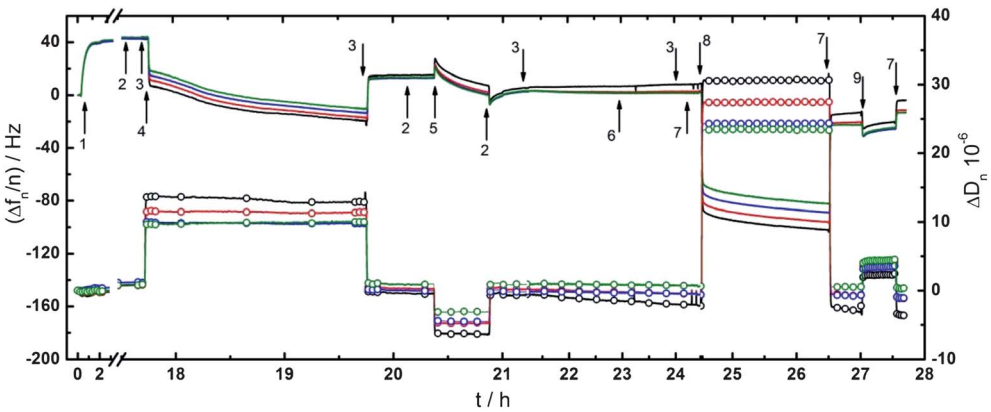

Fig. 3 QCM-D *in situ* response given by $\Delta f_n/n$ (lines, left axis) and ΔD_n (line + symbols, right axis) at overtones (n) of 5 (black), 7 (red), 9 (blue), and 11 (green) for the five steps involved in the modification of the gold substrates: (I) cysteamine in absolute ethanol (arrow 1); (II) glutaraldehyde in pyridine buffer (arrow 4); (III) Ac_2O in absolute ethanol (arrow 5); (IV) aqueous solution of $NaBH_4$ (arrow 6); and (V) aqueous solution of Ni(II) (arrow 8). The last step represents the addition of a 0.2 mol L^{-1} His solution (arrow 9). Arrows 2, 3 and 7 indicate the addition of absolute ethanol, pyridine buffer, and water, respectively.

The modification steps were performed *in situ* with the QCM-D at various overtones (n). In Fig. 3, the normalized change in the resonance frequency ($\Delta f_n/n$) is shown on the left (lines), while the change in the dissipation (ΔD_n) is shown on the right (symbols + lines) for $n = 5$, 7, 9, and 11. In general, a decrease in $\Delta f_n/n$ indicates the mass on the substrate increased, whereas constant values of ΔD_n and signals that do not spread out for the different overtones are clear indications that an acoustically rigid film is formed on the substrate. A duplicate experiment was performed, as shown in the ESI (Fig. S1†), using KNO_3 solution (instead of His) at the end of the experiment. This last step was intended to check the strength of the Ni(II) interaction with the COO-functionalized substrate.

The first step, which is indicated by arrow 1, involved the overnight incubation of the substrate in a cysteamine solution to induce the formation of the amino-SAM. The experimental results indicate that the first step of the modification resulted in an acoustically rigid SAM and occurred with a loss of mass. Z. Cao *et al.* reported that alkanethiol adsorption induces a corrosive oxidation of gold in the presence of oxygen.[34] Despite the monolayer formation, oxygen molecules reacted with the substrate and formed alkane sulfonate or thiolate species, which caused defects to be formed on the gold. The frequency response stabilized at a value of *ca.* 40 Hz after 3 hours of incubation and remained stable after the addition of absolute ethanol (arrow 2) and pyridine buffer (arrow 3). In agreement with SERS spectra, this result indicates that the amino-terminated monolayer was not removed from the substrate after the rinsing steps.

The second step was the reaction between the surface amino groups with glutaraldehyde (arrow 4) to graft the aldehyde functionality onto the substrate that was easily oxidized to produce the carboxylate surface groups. Subsequently, the modified substrate was rinsed with pyridine buffer (arrow 3). The changes in the resonance frequency and dissipation indicate that the mass on the substrate increased and an acoustically viscoelastic process occurred. Upon addition of pyridine buffer, the resonance frequency increased and stabilized at a value of 10 Hz. The initial value of $\Delta f_n/n$ was 40 Hz; therefore, the first two modification steps produced a net decrease of 30 Hz. Considering the initial and final states, the formed Au/Cyst + Glut film was acoustically rigid. To determine if the proposed chemical reactions occurred, QCM-D control experiments were performed, which skipped the first cysteamine step, as shown in the ESI (Fig. S2†). Notably, in the absence of cysteamine (*i.e.*, without the possibility of a covalent reaction between amino and aldehyde groups) approximately the same $\Delta f_n/n$ and ΔD_n profiles were measured ($\Delta f_n/n = 40$ Hz between the initial and final states), which indicates that glutaraldehyde also physically interacts with the gold substrate. The polymerization of glutaraldehyde is known to occur in alkaline media,[35] which can result in the formation of an acoustically rigid film on the substrate in the absence of cysteamine. This physically adsorbed glutaraldehyde may provide the required rigidity to induce the *gauche*/*trans* orientation change observed by SERS.

As indicated in Fig. 3, the addition of Ac_2O (arrow 5) was performed immediately after the addition of absolute ethanol (arrow 2). Similar to the previous step, the process was acoustically viscoelastic; however, the resultant film became rigid after washing (absolute ethanol followed by pyridine buffer). Similar profiles were also observed on physically adsorbed polymeric glutaraldehyde (see Fig. S2, ESI†), which indicates that Ac_2O interacts with unreacted amino groups and the polymeric film. However, the changes in $\Delta f_n/n$ (both before and after washing with absolute ethanol) were more prominent if cysteamine was present ($\Delta f_n/n$ *ca.* −10 Hz) than for the glutaraldehyde polymeric film (Δf_n *ca.* −5 Hz), which indicates that Ac_2O was weakly bound to the polymeric film. An extra experiment (see Fig. S3, ESI†) performed by exposing a Au/Cyst substrate to Ac_2O for 4 hours caused a larger net change to be observed in the resonance frequency ($\Delta f_n/n$ was *ca.* −20 Hz between the initial and final states). In this experiment, all the surface amino groups were available to react with the Ac_2O. A comparison between the net frequency changes in the presence and absence of glutaraldehyde indicates that the amount of Ac_2O on the surface was twice the amount in the case where glutaraldehyde was absent. Fig. S3 (ESI†) also indicates that Ac_2O neither interacts nor reacts with the gold substrate within a 40 minute incubation period.

The fourth step involved the reduction of the imine bond on the Au/Ac_2O + Glut with $NaBH_4$ (arrow 6) (Fig. 3), which was allowed to react for 3 hours. After completion, the Au/COO was washed with the pyridine buffer (arrow 3). The entire step resulted in no change in the resonance frequency ($\Delta f_n/n \sim 0$ Hz), which was comparable to the observed response with the physically adsorbed glutaraldehyde film under the same conditions (see Fig. S2, ESI†). Finally, in the fifth step, the Au/COO was immersed in a 1.0 mol L^{-1} Ni(II) solution (arrow 8) for 2 hours, after the Au/COO was stabilized with water (arrow 7) (Fig. 3). As observed in the other steps, the process was viscoelastic during the incubation, and then the film was acoustically rigid after being washed with water. The net $\Delta f_n/n$ for this process was *ca.* −25 Hz for the film containing cysteamine. Similar profiles were observed for Ni(II) added to the modified gold in the absence of cysteamine, indicating that the Ni(II) cations incorporate into the polymeric film as well as form surface complexes. In this case the net $\Delta f_n/n$ was *ca.* −37 Hz (see Fig. S2, ESI†). On the other hand, Ni(II) was partially removed from the modified substrate upon the addition of His (arrow 9) (Fig. 3) when the modification began with cysteamine as shown by the positive $\Delta f_n/n$ change (*ca.* 9.7 Hz). In the case of the polymeric film with glutaraldehyde, Ni(II) species were not removed either with KNO_3 or with His solution as it can be seen from the similar $\Delta f_n/n$ values before and after the addition of His or KNO_3 (Fig. S2, ESI†). This behavior suggests that Ni(II) cations only are available to react with His-tag protein when the substrate modification begins with cysteamine since they are incorporated in the polymeric glutaraldehyde film.

In summary, QCM-D indicated that two different films were formed: a COO-terminated SAM, which resulted from the oxidation of previously incorporated surface aldehyde groups, and a physically adsorbed polymeric glutaraldehyde film, which was produced in the alkaline medium. The COO-terminated SAM formed a high affinity surface chelation complex with

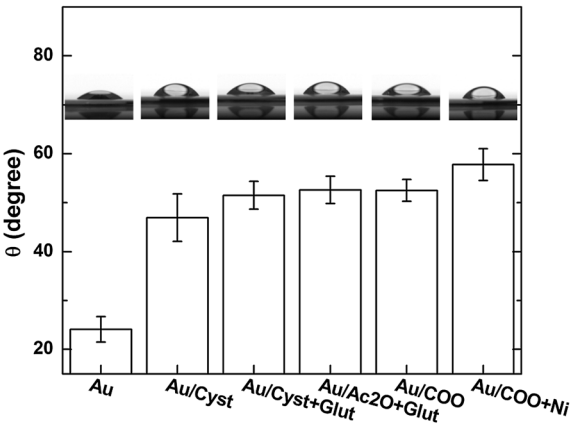

Fig. 4 Contact angle of 5 μL of deionized water on the substrate, which was measured in quadruplicate for all steps in the surface modification process. Surface COO–Ni(II)–His_6 chelate complex.

Ni(II), which was exposed to the solution to be partially disrupted by adding competitor agents, such as His solutions. On the other hand, Ni(II) was not available to react or to be removed when incorporated into the polymeric film.

This multi-step process used to modify the gold substrates was also used on silica substrates, except that APTMS was substituted for cysteamine in the first step. This versatility is one of the major advantages of the multi-step strategy. The formation of amino-terminated SAMs on substrates has been used to graft other functionalities on gold and silica[36] as well as magnetite nanoparticles,[37] plastic[38] and graphite.[39] The same modification principle has been used to graft EDTA on gold[40] and NTA on different substrates.[41,42]

Fig. 4 shows the changes in the hydrophilicity of the substrate after each modification step by measuring the contact angle of a 5 μL drop of water. Bare gold causes the water to have a contact angle of 24° (±3°), which increased to 47° (±5°) after the cysteamine modification. In this case, the hydrophilicity decreased due to the addition of an organic monolayer on the substrate. Notably, the film remained hydrophilic (*i.e.*, $\theta < 90°$). The three subsequent modifications did not change the contact angle, which remained at approximately 50°. This result indicated that the formation of the polymeric glutaraldehyde film did not change the hydrophilicity of the substrate. After the addition of Ni(II), the contact angle became 58° (±3°).

Table 1 shows the ligands and the donor functional groups (as a function of the pH and metal to ligand ratio) involved in the coordination of the Ni(II) cation in the complexes selected to measure as reference spectra.[43,44] Fig. 5A shows the reference XANES spectra (shifted in the *y* axis for clarity), and the corresponding pre-edge peaks are expanded in Fig. 5B. An intense absorption edge at 8341 eV, which is typical for the Ni(II) oxidation state, and a weak pre-edge peak centered at 8332 eV, which is characteristic of the Ni(II) octahedral geometry with a coordination number 6, can be observed in all of the reference spectra. Although the features of the main absorption bands were similar for all of the reference spectra, there were subtle variations at the higher energy side (a broadening and a weakening shoulder), which indicates that differences were present in the electronic environment and coordination sphere of the cation.[19] For example, the spectra of $Ni(NH_3)_6$ and $Ni(His)_2$ show similar variations (*i.e.*, as the water molecules are replaced by other ligands, a slight distortion in the geometry occurs).

Fig. 6A shows the XANES spectra of the Ni complex with acetic acid in aqueous solution as well as the surface complexes

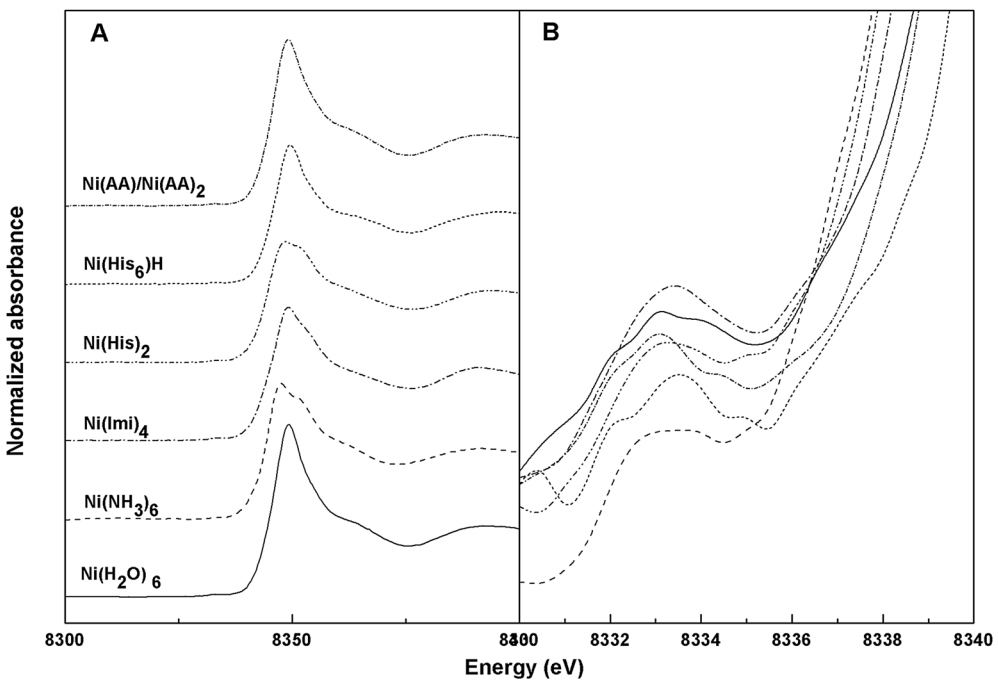

Fig. 5 (A) XANES spectra of the reference complexes in aqueous solution. (B) Pre-edge peak of the spectra shown in (A).

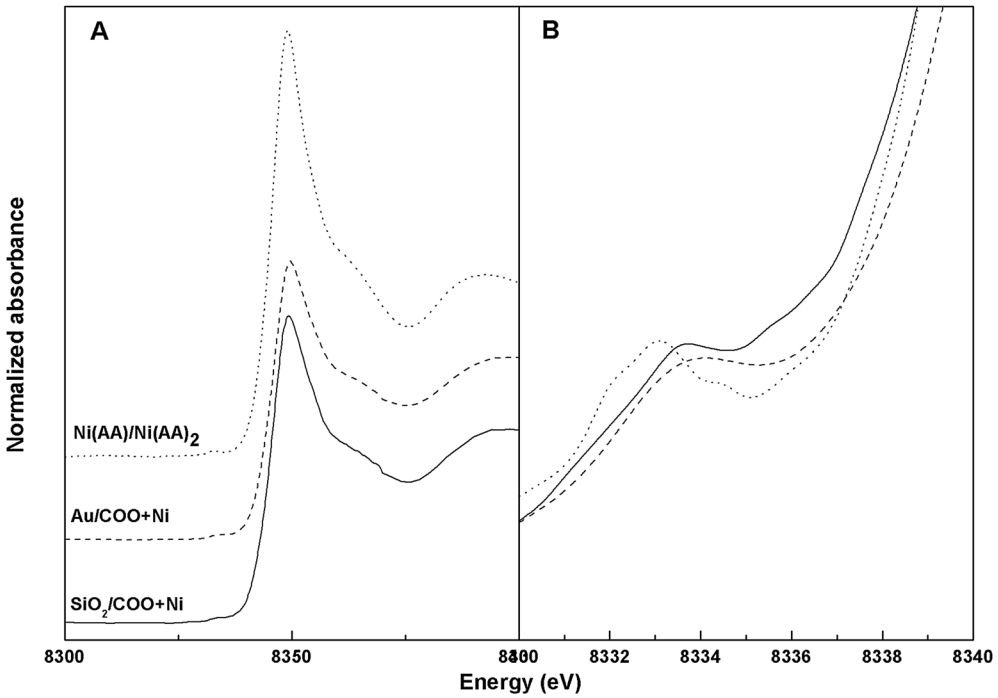

Fig. 6 (A) XANES spectra of the surface complexes. (B) Pre-edge peak of the spectra shown in (A).

on gold (Au/COO + Ni) and silica (SiO_2/COO + Ni) substrates (the spectra are shifted in the *y* axis for clarity). The corresponding pre-edge peaks are expanded in Fig. 6B. Similar to the reference spectra shown in Fig. 5A, the main absorption band of both the Au/COO + Ni and SiO_2/COO + Ni spectra was centered at 8341 eV, which indicates that Ni(II) was present on the surface. Only one weak pre-edge peak centered at 8332 eV was observed, which indicated that the geometry of the complex on the surface was octahedral. The spectra of the surface complexes Au/COO + Ni and SiO_2/COO + Ni had similar features, which indicated that the surface complexes were equivalent regardless of the substrate material used. Comparing the main features of COO–Ni(II) spectra in aqueous solution with those on the substrates (*i.e.*, the position and shape of the absorption edge,

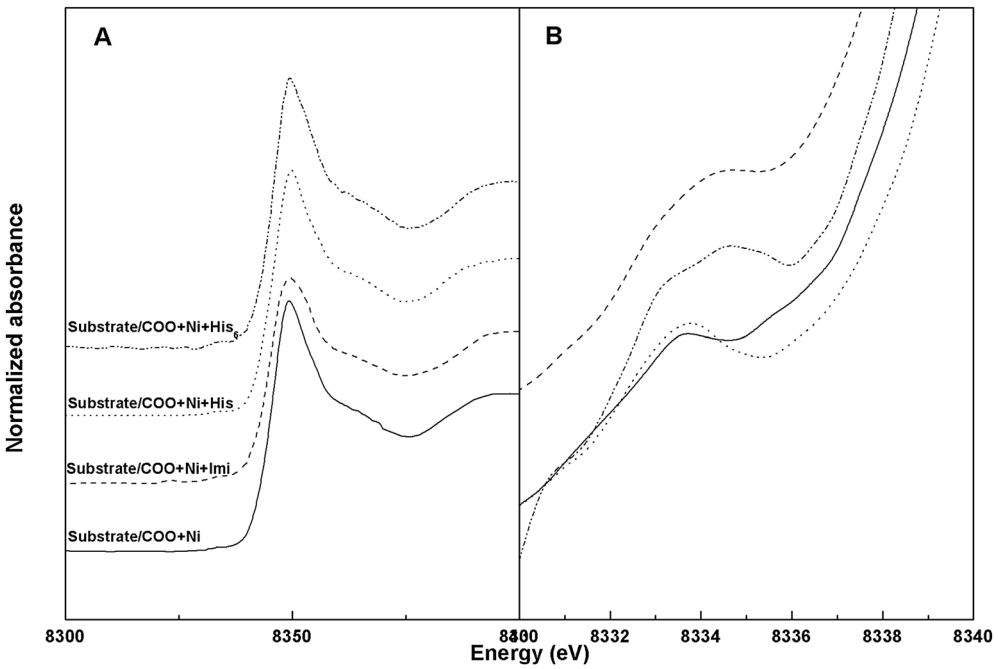

Fig. 7 (A) XANES spectra of the surface complexes. (B) Pre-edge peak of the spectra shown in (A).

the presence of pre-edge peaks and the absence of an increase of width for the main absorption band) resulted in the conclusion that the complexes have the same type of coordination. Therefore, the surface COO–Ni(II) complex had a non-distorted octahedral geometry, which demonstrates that the surface restriction and the chemical modification that joins the COO^- group to the substrate did not modify the electronic environment and coordination sphere of the cation.

Fig. 7A shows the XANES spectra of the surface COO–Ni(II) complexes (substrate/COO + Ni) prior to any further reactions and after the reaction with Imi (substrate/COO + Ni + Imi), His (substrate/COO + Ni + His) or His_6 (substrate/COO + Ni + His_6). The corresponding pre-edge peaks are expanded in Fig. 7B. A main band centered at 8342–8344 eV and one pre-edge peak at 8332–8333 eV can be observed in all of the spectra. Although the features of the main absorption band and pre-edge peak represent hexacoordinated Ni(II) ions, slight spectral changes can be observed, which indicates that differences in the electronic environment and octahedral coordination sphere of the Ni(II) were present.[19] Compared to substrate/COO + Ni(II), the main absorption bands of substrate/COO + Ni + Imi and substrate/COO + Ni + His_6 were broader and a weak shoulder was observed at the higher energy side, which was indicative of the complete removal of water from the complex. Therefore, both Imi and His_6 replaced the water molecules in the two remaining coordination sites of the COO–Ni(II) chelate. However, the substrate/COO + Ni + His spectrum was similar to that of the substrate/COO + Ni, both in intensity and symmetry. This result indicates that the His acted as a monodentate ligand and did not remove all the water molecules coordinated to the COO–Ni(II) complex on the substrate. The similarity between the substrate/COO + Ni + Imi and substrate/COO + Ni + His_6 spectra indicates that His_6 coordinates to the COO–Ni(II) on the surface through the imidazole nitrogen, which is the coordination site of Imi (see Table 1). The spectral changes for the substrate/COO + Ni + His_6 represent the coordination mechanism that occurs as His-tag proteins are added to COO-modified substrates in an aqueous solution: the water-occupied sites of the surface COO–Ni(II) chelate are replaced by the His residues of the adsorbing protein. As indicated in Table 1, His behaves as a tridentate ligand in aqueous solution, in which the carboxyl oxygen (^-OOC), the imidazole nitrogen ($-N_{(Imi)}$) and the amino nitrogen ($-NH_2$) coordinate to Ni(II) ions in an octahedral geometry. There is only one octahedral species between His_6 and Ni(II) ions in the aqueous solution, in which the N-terminal imidazole nitrogen and the adjacent amide nitrogen are coordinated with the cation.[44] However, as His_6 approaches the COO–Ni(II) modified substrate, only the more available imidazole groups replaced the water molecules.

Notably, the XANES results obtained for COO–Ni(II) complexes at the surface in the presence of Imi, His or His_6 indicate that the chelation was highly stable, especially compared to the tridentate iminodiacetic acid (IDA) ligand.[45] Kronina *et al.*[46] reported that His_6 removes Cu(II) from the Cu-IDA modified substrate. However, Ni(II) leakage from the COO-modified substrate (if any) would be low. Furthermore, His_6 was removed from COO–Ni(II)–His_6 upon washing with a concentrated His or Imi solution (data not shown), which indicates that the modified substrate was reusable. A similar behavior was observed with a His-tag antigen adsorbed on this platform.[47]

Electrochemical response

CV experiments were conducted to evaluate the electrochemical stability and response of the modified substrates. Fig. 8 shows the first two cycles of CV measurements for Au, Au/Cyst (A), Au/COO (B), and Au/COO + Ni electrodes (C) in a 50 mmol L^{-1} phosphate buffer at pH 8.0 with a scan rate of 100 mV s^{-1} between 0.00 and 0.70 V. Although this potential window corresponds to the region between the oxidative and reductive SAM desorption (see Fig. S4, ESI†), the electrochemical stability of gold modified with cysteamine was low at potentials higher than 0.40 V. In contrast, the modification processes up to the last step stabilized the Au–SAM interaction, which resulted in a wider available potential range to electrochemically detect biorecognition events. The COO–Ni(II) complexes at the surface were not affected by the applied potential (see Fig. S5, ESI†),

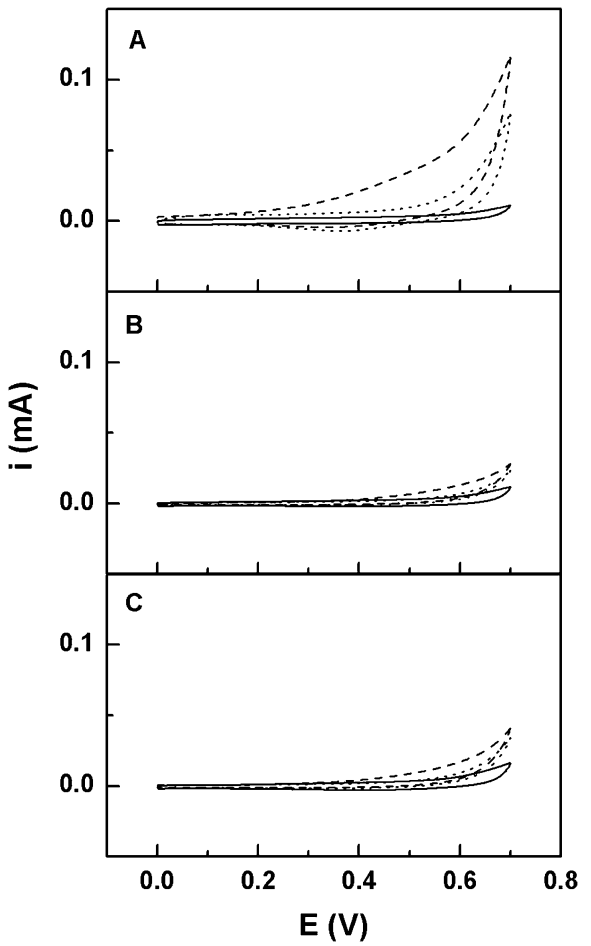

Fig. 8 Voltammograms of bare (solid line) and modified gold after the first (dashed line) and second (dotted lines) scans performed with Au/Cyst (A), Au/COO (B), and Au/COO + Ni (C) electrodes in a 50 mmol L^{-1} phosphate buffer at pH 8.0 at a scan rate of 100 mV s^{-1}.

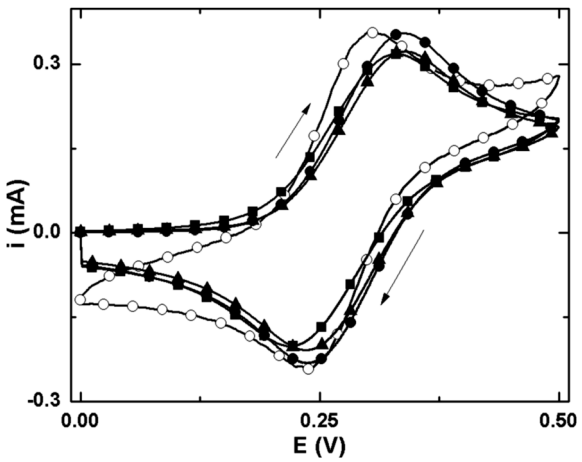

Fig. 9 CV of Au (○), Au/Cyst (■), Au/COO (▲), and Au/COO + Ni (●) electrodes in a phosphate buffer at pH 8.0 with 2.5 mmol L^{-1} Fc at a scan rate of 100 mV s^{-1}.

which indicates that the His-tag proteins will remain attached to the substrate under these experimental conditions.

Fig. 9 compares the voltammograms of Au, Au/Cyst, Au/COO, and Au/COO + Ni electrodes in the presence of 2.5 mM (dimethylamine)ferrocene (Fc) at pH 8.0 (phosphate buffer) at 100 mV s^{-1}. Well-defined redox current peaks corresponding to the Fc/Fc^{+} redox transformation with a peak separation of ~60 mV were observed in the voltammogram of the gold electrode, which was indicative of an electrochemically reversible one-electron process. The peak separation for the gold electrodes modified with cysteamine, COO and COO–Ni(II) was greater than 100 mV. These values can be explained by the decrease of electron-transfer kinetics through the SAM-modified electrode. The SAM clearly had numerous defects (*e.g.*, pinholes). A comparison of the SAMs with cysteamine and other molecular units with extended carbon chains clearly shows that cysteamine-modified gold has more defects, which allows the charge transfer reaction to occur.[7,40,48–51] Consequently, the redox probe can penetrate the SAM to some extent. The SAM acts as a physical barrier and repulsion barriers due to the electrostatic interaction between the amino-terminated SAM and the tertiary amine group of the Fc probe. Therefore, the modification layer is semi-permeable to water and larger molecules such as the redox probe used in this report.

Conclusions

The multi-step strategy used to modify solid substrates (either gold or silica) to build bio-platforms based on His-tag proteins was simple, versatile and highly stable toward washing and applied electric potentials. This modification resulted in a COO–Ni(II)-terminated SAM and the formation of a polymeric glutaraldehyde film. The polymeric glutaraldehyde film physically incorporated Ni(II). The film did not affect the surface properties (*e.g.*, hydrophilicity) and did not interfere with the electrochemical response of the gold substrate.

The exposed Ni(II) cations of the SAM are similar to solution-based Ni(II) regarding surface complexation (coordination and geometry) and His binding. The electrochemical stability and electron transfer capabilities of the modified gold substrate implied that this platform could be easily coupled with an electrochemical method to detect bio-recognition events. Finally, the versatility of the method may allow other moieties to be added such as oligoethylene glycol (to prevent non-specific adsorption of His-tag proteins) and/or redox probes (to improve bio-recognition performance).

Acknowledgements

The authors acknowledge CNPq, FAPESP (09/53199-3), FonCyT (PICT 2007-695), SeCyT-UNC (05/C511) and CONICET (PIP 2010 11220090100672) for financial support. VLM thanks FAPESP (09/09209-4) and LEV and GEH thank CONICET for fellowships. LNLS (Campinas, Brazil) is gratefully acknowledged for the use of the X-ray absorption facilities.

References

1 E. Hochuli, H. Döbeli and A. Schacher, *J. Chromatogr., A*, 1987, **411**, 177–184.
2 G. B. Sigal, C. Bamdad, A. Barberis, J. Strominger and G. M. Whitesides, *Anal. Chem.*, 1996, **68**(3), 490–497.
3 F. Cheng, L. J. Gamble and D. G. Castner, *Anal. Chem.*, 2008, **80**(7), 2564–2573.
4 R. Valiokas, G. Klenkar, A. Tinazli, A. Reichel, R. Tampé, J. Piehler and B. Liedberg, *Langmuir*, 2008, **24**(9), 4959–4967.
5 J. Fick, T. Wolfram, F. Belz and S. Roke, *Langmuir*, 2010, **26**(2), 1051–1056.
6 C.-H. K. Wang, S. Jiang and S. H. Pun, *Langmuir*, 2010, **26**(19), 15445–15452.
7 V. Balland, S. Lecomte and B. Limoges, *Langmuir*, 2009, **25**(11), 6532–6542.
8 C. E. Giacomelli, L. E. Valenti and M. L. Carot, in *Encyclopedia of Surface and Colloid Science*, ed. P. Somasundaran, Taylor & Francis, Oxford, U.K., 2nd edn, 2012, pp. 1–16.
9 C. Ley, D. Holtmann, K.-M. Mangold and J. Schrader, *Colloids Surf., B*, 2011, **88**(2), 539–551.
10 P. A. Millner, H. C. W. Hays, A. Vakurov, N. A. Pchelintsev, M. M. Billah and M. A. Rodgers, *Semin. Cell Dev. Biol.*, 2009, **20**(1), 34–40.
11 S. Boujday, C. Méthivier, B. Beccard and C.-M. Pradier, *Anal. Biochem.*, 2009, **387**(2), 194–201.
12 O. Du Roure, C. Debiemme-Chouvy, J. Malthête and P. Silberzan, *Langmuir*, 2003, **19**(10), 4138–4143.
13 J. K. Lee, Y.-G. Kim, Y. S. Chi, W. S. Yun and I. S. Choi, *J. Phys. Chem. B*, 2004, **108**(23), 7665–7673.
14 M. Zwahlen, S. Herrwerth, W. Eck, M. Grunze and G. Hähner, *Langmuir*, 2003, **19**(22), 9305–9310.
15 G. J. Colpas, M. J. Maroney, C. Bagyinka, M. Kumar, W. S. Willis, S. L. Suib, P. K. Mascharak and N. Baidya, *Inorg. Chem.*, 1991, **30**(5), 920–928.
16 G. Davidson, S. L. Clugston, J. F. Honek and M. J. Maroney, *Biochemistry*, 2001, **40**(15), 4569–4582.
17 P. E. Carrington, F. Al-Mjeni, M. A. Zoroddu, M. Costa and M. J. Maroney, *Environ. Health Perspect.*, 2002, **110**(s5), 705–708.

18 P. E. Carrington, P. T. Chivers, F. Al-Mjeni, R. T. Sauer and M. J. Maroney, *Nat. Struct. Mol. Biol.*, 2003, **10**(2), 126–130.
19 G. Hall, *Geochim. Cosmochim. Acta*, 2004, **68**(17), 3441–3458.
20 H.-c. Huang, Y.-l. Wei, Y.-w. Yang and J.-f. Lee, *J. Electron Spectrosc. Relat. Phenom.*, 2005, **147**(3), 825–828.
21 L. E. Valenti, P. A. Fiorito, C. D. García and C. E. Giacomelli, *J. Colloid Interface Sci.*, 2007, **307**(2), 349–356.
22 T. M. McIntire, S. R. Smalley, J. T. Newberg, A. S. Lea, J. C. Hemminger and B. J. Finlayson-Pitts, *Langmuir*, 2006, **22**(13), 5617–5624.
23 C. Alonso, R. C. Salvarezza, J. M. Vara, A. J. Arvia, L. Vazquez, A. Bartolome and A. M. Baro, *J. Electrochem. Soc.*, 1990, **137**(7), 2161–2166.
24 Z. Q. Tian, B. Ren and D. Y. Wu, *J. Phys. Chem. B*, 2002, **106**(37), 9463–9483.
25 G. Sauerbrey, *Zeitschrift für Physik A Hadrons and Nuclei*, 1959, **155**(2), 206–222.
26 H. Tolentino, J. C. Cezar, D. Z. Cruz, V. Compagnon-Cailhol, E. Tamura and M. C. Martins Alves, *J. Synchrotron Radiat.*, 1998, **5**(3), 521–523.
27 A. Michota, A. Kudelski and J. Bukowska, *Surf. Sci.*, 2002, **502–503**, 214–218.
28 A. Kudelski, *Vib. Spectrosc.*, 2005, **39**(2), 200–213.
29 H. Ju, Y. Xiao, X. Lu and H. Chen, *J. Electroanal. Chem.*, 2002, **518**(2), 123–130.
30 E. Podstawka, Y. Ozaki and L. M. Proniewicz, *Appl. Spectrosc.*, 2005, **59**(12), 1516–1526.
31 M. Yuan, S. Zhan, X. Zhou, Y. Liu, L. Feng, Y. Lin, Z. Zhang and J. Hu, *Langmuir*, 2008, **24**(16), 8707–8710.
32 E. Podstawka, Y. Ozaki and L. M. Proniewicz, *Appl. Spectrosc.*, 2004, **58**(5), 570–580.
33 M. B. Smith, in *March's Advanced Organic Chemistry: Reactions, Mechanisms, and Structure*, John Wiley & Sons, New Jersey, U.S.A., 7th edn, 2013.
34 Z. Cao, L. Zhang, C.-Y. Guo, F.-C. Gong, S. Long, S.-Z. Tan, C.-B. Xia, F. Xu and L.-X. Sun, *Mater. Sci. Eng., C*, 2009, **29**(3), 1051–1056.
35 a. Jayakrishnan and S. R. Jameela, *Biomaterials*, 1996, **17**(5), 471–484.
36 J. Kim, J. Cho, P. M. Seidler, N. E. Kurland and V. K. Yadavalli, *Langmuir*, 2010, **26**(4), 2599–2608.
37 Y. Liao, Y. Cheng and Q. Li, *J. Chromatogr., A*, 2007, **1143**(1–2), 65–71.
38 J. Maly, E. Illiano, M. Sabato, M. De Francesco, V. Pinto, a. Masci, D. Masci, J. Masojidek, M. Sugiura, R. Franconi and R. Pilloton, *Mater. Sci. Eng., C*, 2002, **22**(2), 257–261.
39 J. Maly, C. Di Meo, M. De Francesco, a. Masci, J. Masojidek, M. Sugiura, a. Volpe and R. Pilloton, *Bioelectrochemistry*, 2004, **63**(1–2), 271–275.
40 R. K. Shervedani, A. Farahbakhsh and M. Bagherzadeh, *Anal. Chim. Acta*, 2007, **587**(2), 254–262.
41 R. K. Shervedani and M. Bagherzadeh, *Electrochim. Acta*, 2008, **53**(22), 6293–6303.
42 Y. C. Liu, N. Rieben, L. Iversen, B. S. Sørensen, J. Park, J. Nygård and K. L. Martinez, *Nanotechnology*, 2010, **21**(24), 245105.
43 S. Kotrly and L. Sucha, *Handbook of Chemical Equilibria in Analytical Chemistry*, Ellis Horwood Limited, 1985.
44 L. E. Valenti, C. P. De Pauli and C. E. Giacomelli, *J. Inorg. Biochem.*, 2006, **100**(2), 192–200.
45 L. C. de Góes, E. A. Miranda and S. M. A. Bueno, *Colloids Surf., A*, 2010, **369**(1–3), 176–185.
46 V. V. Kronina, H.-J. Wirth and M. T. W. Hearn, *J. Chromatogr., A*, 1999, **852**(1), 261–272.
47 L. E. Valenti, A. Smania, C. P. De Pauli and C. E. Giacomelli, *Colloids Surf., B*, 2013, DOI: 10.1016/j.colsurfb.2013.07.059.
48 D. Losic, J. G. Shapter and J. J. Gooding, *Langmuir*, 2001, **17**(11), 3307–3316.
49 M. N. Paddon-Row and J. J. Gooding, *J. Phys. Chem. B*, 2004, **108**(24), 8460–8466.
50 A. Kiani, M. a. Alpuche-Aviles, P. K. Eggers, M. Jones, J. J. Gooding, M. N. Paddon-Row and A. J. Bard, *Langmuir*, 2008, **24**(6), 2841–2849.
51 A. Chou, P. K. Eggers, M. N. Paddon-Row and J. J. Gooding, *J. Phys. Chem. C*, 2009, **113**(8), 3203–3211.
52 T. J. Strathmann and S. C. B. Myneni, *Geochim. Cosmochim. Acta*, 2004, **68**(17), 3441–3458.